

Quantum point contact as a local probe of the electrostatic potential contours

J. G. Williamson and C. E. Timmering

Philips Research Laboratories, 5600 JA Eindhoven, The Netherlands

C. J. P. M. Harmans

Department of Applied Physics, Delft University of Technology, 2600 GA Delft, The Netherlands

J. J. Harris and C. T. Foxon

Philips Research Laboratories, Cross Oak Lane, Redhill, Surrey RH1 5HA, United Kingdom

(Received 11 July 1990)

Quantum point contacts, shifted laterally by ± 50 nm have been used to study the local electrostatic potential in the two-dimensional electron gas of a GaAs-Al_xGa_{1-x}As heterostructure. The resistance of the quantized plateaux is observed to vary with this lateral position. In one device an alternate suppression of the quantized resistance plateaux is observed, which we interpret as being due to an overlap of strong local potential fluctuations with the transverse profile of the wave functions in the quantum point contact.

The last few years have seen many new results in the quantum ballistic transport regime in the high-mobility two-dimensional electron gas (2D EG) of a GaAs-Al_xGa_{1-x}As heterostructure.¹ It has recently become clear that the precise form of current and voltage probes are crucial to the properties of the structure under study.² Nixon and Davies have recently emphasized the importance of local potential fluctuations, which are present naturally because of inhomogeneities in the distribution of ionized impurities.³ Washburn *et al.* have invoked such fluctuations as a possible explanation for conductance fluctuations in a narrow channel containing a potential barrier.⁴ In light of these developments it is clearly desirable to develop techniques to study the properties of individual current-carrying states⁵ and the potential landscape through which they propagate directly, without introducing intrusive voltage probes to the system under study. Recently Glazman and Larkin have calculated⁶ that the confining potential of a quantum point contact^{7,8} can be shifted laterally with little change in shape, by applying a different voltage on the two halves of the split gate. In this paper we employ this method to study the local potential landscape. We observe that the value of the resistance on a plateau can vary significantly as the point contact is shifted laterally, indicating that there is a series resistance contribution originating locally (and not in the wide 2D EG or contact regions). Also data is presented showing quantized conductance plateau corresponding alternately to odd or even multiples of $2e^2/h$ as the quantum point contact is shifted laterally.⁹ We interpret this as being due to an overlap of the transverse profile of the one-dimensional wave functions with strong local fluctuations in the potential landscape.

The structure, which has been described more completely elsewhere,¹⁰ consisted of two adjacent quantum point contacts, defined electrostatically by means of split Schottky gates in the 2D EG of a GaAs-Al_xGa_{1-x}As heterostructure. The heterostructure material consisted of a thick GaAs layer, a 40-nm undoped Al_xGa_{1-x}As spacer

layer, a 38-nm Al_xGa_{1-x}As layer doped with silicon at $1.33 \times 10^{24} \text{ m}^{-3}$, and a 17-nm GaAs capping layer. The electron density was $2.0 \times 10^{15} \text{ m}^{-2}$, the Fermi energy was 7 meV, and the transport mean free path was 7 μm . The opening between the gates defining the point contact was about 400 nm. All experiments were carried out at a temperature of 1.5 K. Measurements were made using a low-frequency ac lock-in technique, with $V_{\text{rms}} < 25 \mu\text{V}$. We define the gate-voltage difference $\Delta V_g = V_1 - V_2$ and the average gate voltage $\bar{V}_g = (V_1 + V_2)/2$, where V_1 and V_2 are the voltages on the two half gates (see inset in Fig. 4). A 3D plot of resistance versus ΔV_g and \bar{V}_g is shown in Fig. 1. The step in ΔV_g was 0.02 V and that in \bar{V}_g 0.01 V. Clearly for a given ΔV_g , the resistance as a function of \bar{V}_g is that characteristic of a quantum point contact, where for a standard quantized conductance plot $\Delta V_g = 0$. For a constant average gate voltage \bar{V}_g , varying ΔV_g has the effect of scanning the potential distribution due to the gate laterally over the 2D EG.⁶ We note the following features: close to $\Delta V_g = 0$ the quantized plateau corresponding to $n = 1$ is absent, the quantized resistance plateaux do not run parallel to ΔV_g , and the onset value of a given plateau varies by up to 10% of \bar{V}_g for different ΔV_g . After thermal cycling to 300 K the detailed plot structure was altered. In particular, the plateaux became virtually parallel to the ΔV_g axis, suggesting that the plateau misalignment mentioned above did not arise solely from asymmetries in the gate pattern. The observed resistance fluctuations were also about a factor of 2 smaller and the $n = 1$ plateau was well defined over the whole plot. Taken together these features suggest that the variations in resistance as a function of ΔV_g observed in Fig. 1 arose from variations in the random ionized donor distributions rather than physical defects in the gate, growth defects, or GaAs-Al_xGa_{1-x}As interface irregularities.

We now turn to a quantitative estimate of the spatial extent of the lateral scan and the effect of the potential landscape on the energy levels in the quantum point contact. The lateral position of the potential minimum x_{min} ,

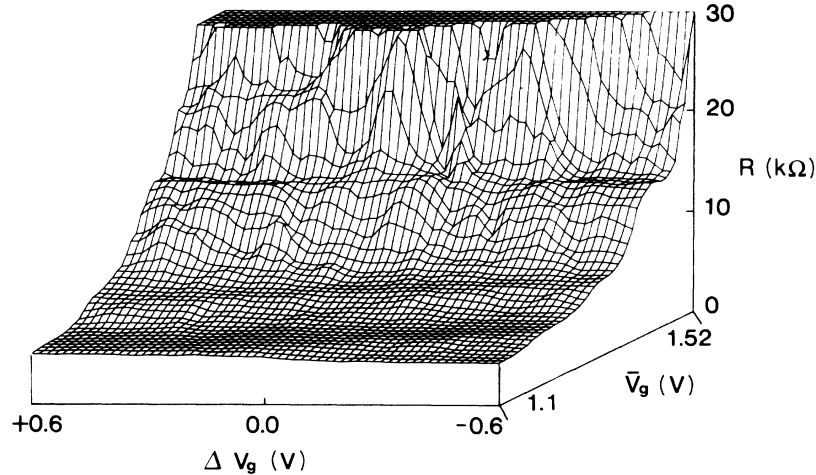


FIG. 1. The resistance of a quantum point contact as a function of the average \bar{V}_g , and difference ΔV_g of the voltages on the two halves of the split gate.

between two infinitely long colinear wires at voltages V_1 and V_2 separated by an opening $2s$ is

$$x_{\min} = s(V_1 - V_2)/(V_1 + V_2). \quad (1)$$

For our configurations this implies a lateral shift of ± 50 nm at $\bar{V}_g = 1.2$ V, $\Delta V_g = \pm 0.6$ V (cf. the circle in the inset in Fig. 4). We have confirmed that this shift was also realized experimentally by using an electron focusing technique⁵ to measure the variation in the spacing between two point contacts.

To estimate the energy of the bottom of each subband, we have fitted the observed resistance variations in \bar{V}_g by modeling the confining potential as parabolic. We assume further that the potential simply scales with applied gate voltage \bar{V}_g so that the potential distribution P due to the gates may be written as

$$P(x) = [\frac{1}{2}a_2(x - x_{\min})^2 + a_0]\bar{V}_g. \quad (2)$$

To extract a_2 and a_0 we assume that the energy of the n th subband corresponds to the Fermi energy at a gate voltage midway between the n th and the $(n+1)$ th plateaux. A fit to a typical data set, near to $\Delta V_g = 0$, yields for the energy of the n th subband

$$E_n = [4.2\bar{V}_g \text{ V}^{-1} + 0.55(n - \frac{1}{2})](\bar{V}_g)^{1/2} \text{ V}^{-1/2}] \text{ meV} \quad (3)$$

and gives $a_0 = 4.2 \text{ meV V}^{-1}$ and $a_2 = 1.33 \times 10^{14} \text{ meV m}^{-2} \text{ V}^{-1}$. The constants in Eqs. (2) and (3) depend on both the particular device used and on ΔV_g , but roughly similar values were found for fits to all devices studied for all ΔV_g , and so we have used these as an estimate of the quantum point contact potential for all data presented here. Within the limitations of this assumption, we can extract the underlying potential-energy variations from the average gate voltage required to define subsequent conductance plateaux, with a spatial resolution which is determined by the parameters of the point-contact confining potential. We thus use the point contact itself, rather than an intrusive "voltage" probe, to gain information about the local electrostatic potential. Inspection of Fig. 1 reveals that typical plateau onset changes at

$\bar{V}_g = 1.3$ V are about 0.08 V for $\Delta V_g = \pm 0.6$ V. Note that this change cannot arise simply from the inclusion of a linear term in Eq. (2), proportional to $|\Delta V_g|$, which will lead to a small reduction in the underlying potential due to the gates, since this should give rise to a symmetric drop around $\Delta V_g = 0$ V, which is not observed. We can also exclude some asymmetry in the physical gate pattern, because, as mentioned above, after temperature cycling the quantized plateaux were observed to run almost parallel to the ΔV_g axis. We, therefore, interpret the change in the onset gate voltage, using Eq. (3), to be due to changes in the underlying random potential distribution of approximately 0.4 meV over 100 nm.

Another feature of the data in Fig. 1 is that the resistance of a given plateau can be different for different values of ΔV_g . This is illustrated in Fig. 2 where the resistance as a function of \bar{V}_g is plotted for five values of ΔV_g between -0.5 and -0.6 V and five values between 0.5 and 0.6 V (the data from the extreme right-hand side and left-hand side of Fig. 1). It is clear that, while the plateau corresponding to $n=1$ is well defined in both cases, the plateau level differs by roughly 1.5 k Ω for $\Delta V_g = \pm 0.6$ V.

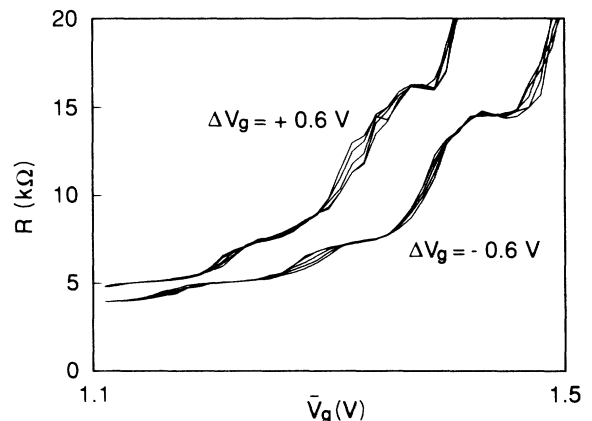


FIG. 2. Resistances as a function of \bar{V}_g for five values of ΔV_g between -0.5 and -0.6 V and 0.5 and 0.6 V.

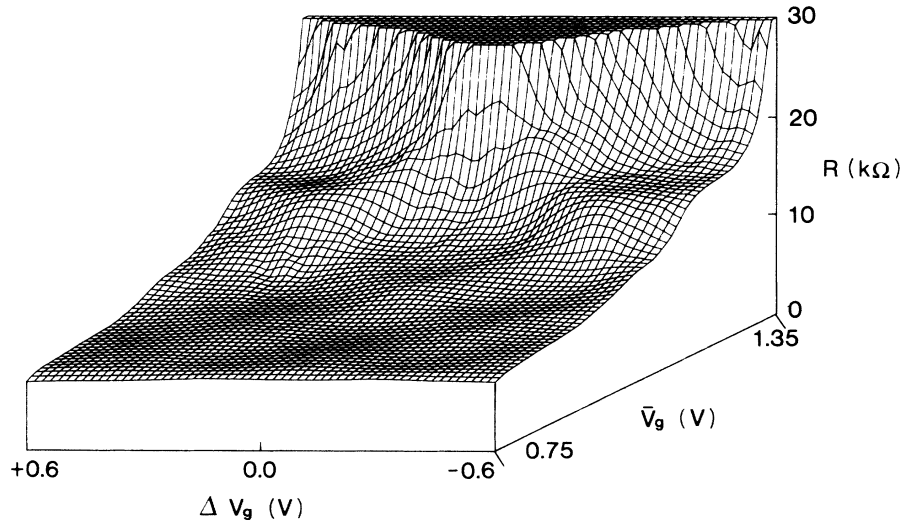


FIG. 3. Plot of resistance vs \bar{V}_g and ΔV_g for another quantum point contact, illustrating the pattern of quantized plateau suppression.

One writes the total resistance on the $n=1$ plateau conventionally as

$$R = R_b + h / (2e^2 T_1), \quad (4)$$

where T_1 is the transmission probability for the $n=1$ subband, and R_b is some small background resistance originating far from the point contact. Note that the same device was used, and thus one may reasonably expect that R_b was constant as a function of ΔV_g . We therefore interpret the plateau resistance change as arising from a change in T_1 of roughly 10% due to local variations in the details of the electrostatic potential landscape between $\Delta V_g = \pm 0.6$ V. It is remarkable that a rather flat plateau is obtained even for nonunit transmission probability. Note also that for small variations in ΔV_g (cf. five superimposed curves in Fig. 2), the plateau levels are virtually unaltered, showing that the subband transmission probability varies slowly under this change. At the same time the conductance between the plateaus shows much larger fluctuations. This suggests that the primary effect on a length scale of tens of nanometers is a change in the underlying potential level rather than a change in the potential shape. We note that this device also exhibited the increase in the “background” resistance with the gate voltage magnitude for different quantized plateaus which has been observed previously.¹¹

In Fig. 3 we show the resistance as a function ΔV_g and \bar{V}_g for a different quantum point contact. One sees two distinct sets of plateaus. For the case where $\Delta V_g \approx 0.06$ V even index plateaus dominate while the odd-numbered plateaus are either weak or absent. For $\Delta V_g = 0.06 \pm 0.36$ V the odd plateaus dominate. We interpret this behavior as being due to a strong potential spike, small enough to resolve the transverse profile of the wave functions and located close to the center of the quantum point contact. In such a system the subband energy shift will depend on the local amplitude of the lateral wave function at the spike. For the case where the spike is at the center of the quantum point contact, one would expect odd modes to be

strongly shifted, and even modes less so. As the point contact position is shifted laterally by one quarter of a transverse wavelength $\lambda_n/4$ of the highest occupied subband, the shifted mode should switch from odd to even. This is demonstrated in Fig. 4 where a “background” subtraction of 1.3 k Ω has been applied. The solid line shows the conductance variation as a function of \bar{V}_g for $\Delta V_g = -0.06$ V. Since the odd index plateaux are virtually absent we conclude that the potential spike is close to the point-contact center. The dashed and dotted lines in Fig. 4 were taken at $\Delta V_g = +0.30$ and -0.42 V, respectively. In both cases only odd index plateaux are present, so that this corresponds to shifts of roughly $\pm \lambda_n/4$ for $n=3$. Note that,

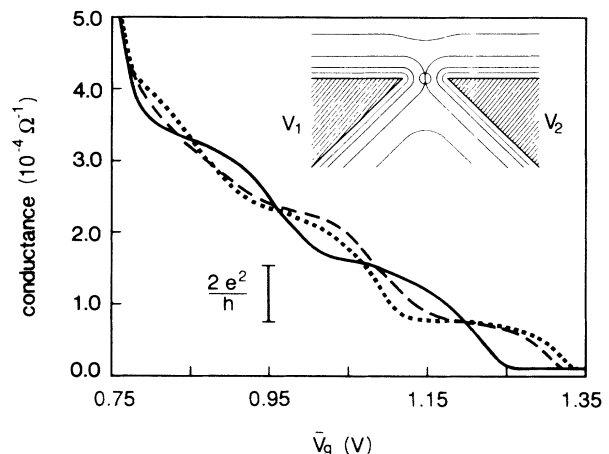


FIG. 4. Conductance plots for $\Delta V_g = -0.06$ V (solid line), $\Delta V_g = +0.30$ V (dashed line), and $\Delta V_g = -0.42$ V (dotted line), for the same data as in Fig. 3, illustrating the suppression of either odd or even index quantized resistance plateaux. Inset: schematic device diagram. The shaded parts indicate the gate used to define the point contacts and the 2D EG boundary, the squares denote the Ohmic contacts, the contours signify the electrostatic potential due to the gate, and the circle represents the area where the lateral scan is carried out.

with this background subtraction, the plateau spacing is approximately $4e^2/h$ (cf. the bar in Fig. 4). Just as with the device discussed above, it is not possible to find a single "background" resistance such that all plateau resistances are perfectly quantized. According to our simple model, the pattern of plateau suppression will depend both on the position of the potential minimum [Eq. (1)], and on its form [Eq. (2)]. We now show that the pattern present in the data is consistent with a resolution of the transverse profile of the confined one-dimensional electron wave functions. In Fig. 3 there are three plateaux at $n=1$ between $0.6 \text{ V} < \Delta V_g < -0.6 \text{ V}$, four plateaux at $n=2$, five at $n=3$, and six at $n=4$. Using Eq. (1) to estimate λ_n , leads to $\lambda_n=200, 150, 120$, and 110 nm for $n=1, 2, 3$, and 4 , respectively. These numbers are consistent with those obtained independently from the shape of the confining potential [Eqs. (2) and (3)], which give $\lambda_n=190, 160, 130$, and 110 nm for $n=1, 2, 3$, and 4 , respectively. This means that the periodicity of the conductance in ΔV_g is $\lambda_n/2$, as one would expect if the wave function profile was resolved.

We do not have a firm candidate for the origin of the strong potential spike. McEuen *et al.* have attributed structure in the conductance of a quantum point contact

below $2e^2/h$ as being due to resonant tunneling through a single impurity ion.¹² Similar structure was observed in one of the experiments; however, this vanished after temperature cycling, while the dominant odd-even plateau switching effect remained.

In conclusion, we have shown that it is possible to measure both local electrostatic potential fluctuations, and the change in transmission probability for a given subband, by scanning a quantum point contact laterally across a 2D EG. For one device we observe a pattern of plateaux suppression which we interpret as being a direct observation of local amplitude variations in the wave functions of laterally confined electrons in a quantum point contact.

The authors would like to thank H. van Houten, C. W. J. Beenakker, J. H. Davies, J. A. Nixon, D. A. Wharam, and M. F. H. Schuurmans for valuable discussions. Financial support was provided by the Stichting voor Fundamenteel Onderzoek der Materie (FOM), The Netherlands and under ESPRIT (the European Strategic Programme of Research and Development in Information Technology) Basic Research Action Project No. 3133 of the Commission of the European Communities, Luxembourg.

¹Nanostructure Physics and Fabrication, edited by M. Reed and W. P. Kirk (Academic, New York, 1989).

²C. J. B. Ford, S. Washburn, M. Buttiker, C. M. Knoedler, and J. M. Hong, Phys. Rev. Lett. **62**, 2724 (1989).

³J. Nixon and J. Davies, Phys. Rev. B **41**, 7929 (1990).

⁴S. Washburn, A. B. Fowler, H. Schmid, and D. Kern, Phys. Rev. B **38**, 1554 (1988).

⁵J. G. Williamson, H. van Houten, C. W. J. Beenakker, M. E. I. Broekaart, L. I. A. Spindeler, B. J. van Wees, and C. T. Foxon, Phys. Rev. B **41**, 1207 (1990).

⁶L. I. Glazman and I. A. Larkin (unpublished).

⁷B. J. van Wees, H. van Houten, C. W. J. Beenakker, J. G. Williamson, L. P. Kouwenhoven, D. van der Marel, and C. T. Foxon, Phys. Rev. Lett. **60**, 848 (1988).

⁸D. A. Wharam, T. J. Thornton, R. Newbury, M. Pepper, H. Ahmed, J. E. F. Frost, D. G. Hasko, D. C. Peacock, D. A. Ritchie, and G. A. C. Jones, J. Phys. C **21**, L209 (1988).

⁹Double-conductance steps have previously been observed in devices with two quantum point contacts in parallel. See C. G. Smith, M. Pepper, R. Newbury, H. Ahmed, D. G. Hasko, D. C. Peacock, J. E. F. Frost, D. A. Ritchie, G. A. C. Jones, and G. Hill, J. Phys. Condens. Matter. **1**, 6763 (1989).

¹⁰H. van Houten, C. W. J. Beenakker, J. G. Williamson, M. E. I. Broekaart, P. H. M. van Loosdrecht, B. J. van Wees, J. E. Mooij, C. T. Foxon, and J. J. Harris, Phys. Rev. B **39**, 8556 (1989).

¹¹D. A. Wharam, M. Pepper, H. Ahmed, J. E. F. Frost, D. G. Hasko, D. C. Peacock, D. A. Ritchie, and G. A. C. Jones, J. Phys. C **21**, L887 (1988).

¹²P. L. McEuen, B. W. Alphenaar, R. G. Wheeler, and R. N. Sacks, in *Proceedings of the Eighth International Conference on Electronic Properties of Two-Dimensional Systems, Grenoble, France, 1989*, edited by J. Y. Marzin, Y. Guldner, and J. C. Maan [Surf. Sci. **229**, 312 (1990)].